Nuclear-structure dependence of the $E1$ strength located in the giant dipole resonance of heavy nuclei

R. Nolte, F. Schröder, A. Baumann, K. W. Rose, K. Fuhrberg, and M. Schumacher

II. Physikalisches Institut der Universität Göttingen, D-3400 Göttingen, Federal Republic of Germany

P. Fettweis* and R. Carchon

Studiecentrum voor Kernenergie–Centre d' Etude de l'Energie Nucleaire, B-2400 Mol, Belgium

Using monochromatic photons from (n,γ) and (p,γ) capture reactions, the elastic scattering of photons was studied in the mass range $A = 181-238$ and energy range $E = 8-18$ MeV. It is shown that the A dependence of the enhancement of $E1$ strength located in the giant-dipole resonance as revealed by part of the photoneutron cross sections is confirmed by our photon-scattering data. The possibility is discussed that the concentration of $E1$ strength in the giant dipole resonance may be larger for closed-shell nuclei as compared to open-shell nuclei.

I. INTRODUCTION

One of the most challenging goals of present day nuclear physics is the detailed understanding of the role subnuclear degrees of freedom play in nuclei. In the conventional picture we are adopting in this work, subnuclear degrees of freedom may be viewed in terms of mesons which are responsible for nuclear forces and for the exchange currents between nucleons and in terms of nucleon excited states. The access to phenomena related to exchange currents is comparatively easy in few-nucleon systems, where detailed calculations are possible. In complex nuclei this task is much more difficult, mainly because of many-body nuclear-structure effects which are coming into play.

One of the most prominent phenomena related to exchange currents is the enhancement of the integrated dipole photoabsorption cross section over the Thomas-Reiche-Kuhn (TRK) sum-rule prediction. Calculations of the enhancement factor κ have been carried out in terms of nuclear forces, acting between nucleons in the nuclear ground state. The first prediction[1] for κ was 0.4 which was realized to be too small by a factor of 2 after photoabsorption measurements had been extended up to the pion threshold.[2-4] A semiquantitative explanation of this discrepancy was obtained, after correlations had been incorporated into the nuclear ground-state wave function.[5,6] Later on, this type of work has been continued by several groups, starting from different ground-state wave functions and using different methods of incorporating the two-nucleon correlations.[7]

In a more ambitious approach to an understanding of the dipole photoabsorption cross section and in order to avoid the closure approximation, we may start from the excitation mechanisms involved in the photoabsorption process, rather than from properties of the nuclear ground state. Simplifying, we may distinguish between only two different modes of excitation, the giant dipole resonance (GDR) and the quasideuteron (QD) mode. In

a shell model for the spherical or deformed nucleus, the GDR corresponds to 1p-1h $1\hbar\omega$ transitions of $E1$ multipolarity[8] whereas the QD excitation corresponds to 2p-2h transitions of proton-neutron pairs, correlated by the exchange of a charged pion.[9,10] It is customarily believed that in case there were no exchange currents, the GDR mode of excitation would exhaust just one TRK sum rule and the QD mode of excitation would not exist. After turning on the exchange currents, the GDR integrated $E1$ strength is enhanced by a factor of $(1+\kappa_{\mathrm{GDR}})$ and the QD mode of excitation contributes an additional amount of κ_{QD} TRK sum rules. To the authors's knowledge this line of thinking has not been worked out quantitatively. There are only few investigation, where κ, calculated in a correlated ground state, is partitioned into two different parts which have been attributed to the GDR and QD effect, respectively.[5,11-13] One motivation for this partition was the prediction that the GDR part κ_{GDR} of κ is of the same physical origin as the mesonic contribution δ_{g_1} to the orbital magnetic moment of the nucleon, whereas the physical origin of the QD part is different.

The purpose of the present work is to get further insights into nuclear dynamics and its interplay with mesonic currents in the GDR mode of excitation. The questions we wish to answer are the following: (i) How large are the enhancements κ_{GDR} over the TRK sum-rule predictions for the $E1$ strengths located in the GDR's of heavy nuclei and (ii) are these enhancements the same for all nuclei, or different, e.g., for closed-shell and open-shell nuclei?

Our method is the elastic scattering of photons produced by neutron and proton capture reactions. Making use of the well-known angular dependence of the elastic differential cross section, corrections to the GDR parameters may be obtained. Our method of using few narrow photon lines and making use of high-resolution Ge(Li) detectors as spectrometers has the advantage of providing very accurate elastic differential cross sections. However, it has the disadvantage of being restricted to heavy

nuclei where—with the exception of ^{208}Pb—the GDR photoabsorption cross section is well represented by one or the superposition of two Lorentzian lines, with little additional structures. The use of Lorentzian representations has the further advantage that the known low-energy and the expected high-energy tails of the GDR are taken into account at least approximately. Preliminary results have been presented in conference reports.[14] Related work has recently been published by Nathan *et al.*[15] carrying out photon scattering experiments on ^{206}Pb using tagged photons, and by Berman *et al.*[16] measuring photoneutron cross sections for Zr, I, Pr, Au, and Pb.

II. EXPERIMENTS

Photon scattering experiments have been carried out at the reactor BR2 of the Belgian nuclear research center Studiecentrum voor Kernenergie–Centre d'Etude de l'Energie Nucleaire (SCK-CEN) in Mol and at the 1-MeV proton accelerator PHOENIX in Göttingen, using photons from neutron and proton capture reactions, respectively. For the reactor experiments, 770 g of Ni containing 2.7 g of ^{59}Ni ($T_{1/2}=7.5\times10^4$ yr) were attached to the outer side of the end plate of an Al tube under vacuum, inserted into the $T8$-$T3$ tangential through hole of the reactor, the latter being filled with water used as coolant for the Ni target and as neutron reflector. Since the Ni target is situated outside of the Be reflector of the reactor, it is submitted to a neutron flux of only 3×10^{12} s^{-1}cm^{-2}. Nevertheless, because of the large mass of the capture target and the high cross sections of ^{59}Ni (92 b) an intense photon beam of discrete γ rays of 8.533, 8.999, and 11.388 MeV was obtained, amounting to 2.0×10^7, 4.5×10^7, and 1.3×10^6 s^{-1} photons on a 120-cm^2 scattering target, respectively. The width of these lines is due to thermal motion only and amounts to $\Delta E\approx20$ eV full width at half-maximum (FWHM) and is thus completely negligible with respect to the resolution of the used Ge(Li) detectors. The 2.7 g of ^{59}Ni were obtained through the ^{58}Ni(n,γ) reaction during a 60 d preirradiation of the Ni target in a high flux region (4.5×10^{14} s^{-1}cm^{-2}) of the reactor.

The scattering arrangement used at the reactor BR2 is depicted in Fig. 1. The photon beam is delimitated by an iron collimator and neutron filtered by borated paraffin. The collimator was 6 cm×6 cm wide, and had a length of 1 m. It was divided into two halves by an iron plate serving as shield against photons coming from the reactor core. The scattering target is positioned between two lead housings, each containing a large-volume Ge(Li) detector. The scattering angle was 135° for both detectors. The housings were covered with borated paraffin serving as a neutron shield. In addition, the Ge(Li) detectors were surrounded by plastic-scintillator veto counters, to suppress the cosmic-ray background. A reduction of cosmic-ray background of more than 83% was achieved. Since the neutron flux in the reactor is not constant, the direct beam was monitored permanently. This was achieved with an additional Ge(Li) detector placed in the direct beam, behind a wall consisting of Pb and paraffin.

The monitor detector was calibrated relative to the detectors of the scattering arrangement, by positioning the latter in the direct beam and comparing the count rates.

Photons of energy 17.64 MeV were produced by resonance capture of 440-keV protons in ^{7}Li. The width of this photon line corresponds to the width of the resonant state being[17] 10.7-keV FWHM. An additional photon line, having a width of 1.45 MeV and an average energy of 14.7 MeV is produced with an intensity of 50% of that of the 17.64-MeV line. The proton capture target consisting of 1 mm of metallic Li on a water-cooled aluminum backing was bombarded with 600-keV protons, which were stopped completely in the Li layer. With a proton current of 550 μA, a flux of photons of 1.0×10^5 s^{-1} was achieved on the scattering target in the arrangement shown in Fig. 2. To maximize the count rate of scattered photons, the distances between source and scatterer and between scatterer and detector were kept as small as possible. Therefore, it was not possible to collimate the beam. Instead a W-Cu-Ni alloy having a density of 18 g/cm^3 was used to effectively shield the Ge(Li) detector from the high flux of photons coming directly
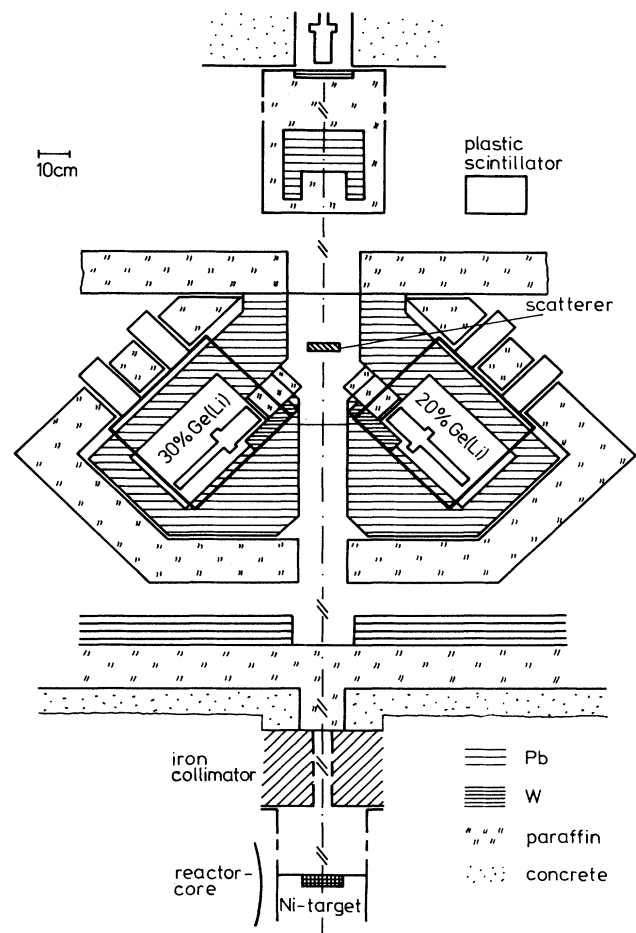

FIG. 1. Experimental setup used at the ^{58,59}Ni(n,γ) photon beam installed at the reactor BR2 in Mol. Two large-volume Ge(Li) detectors are inserted in low-background housings. The cosmic-ray background is suppressed by NE 102 veto counters.
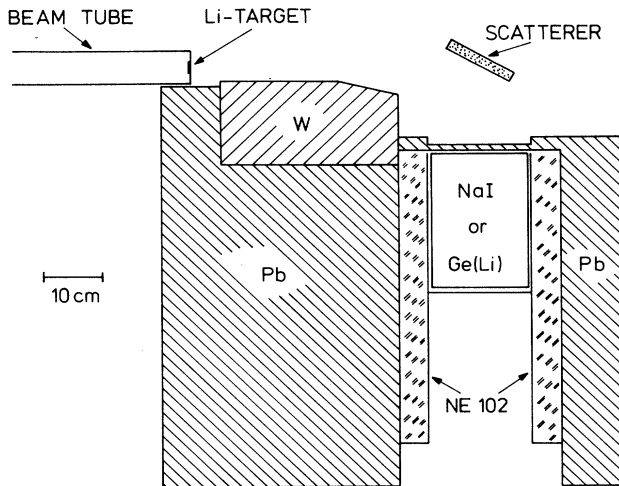
FIG. 2. Experimental setup used at the ^{7}Li(p,γ) photon beam installed at the 1-MeV accelerator PHOENIX in Göttingen. A $16\times16\times24$ cm^3 NaI(Tl) detector or a Ge(Li) detector (30% efficiency compared to 7.6×7.6 cm NaI(Tl) is inserted in a low-background housing. The cosmic-ray background is suppressed by a NE 102 veto counter.

detector. Then by nuclear reactions of fast neutrons and capture of thermalized neutrons in the NaI(Tl) detector background events within the 17.64-MeV photon line may be produced. To discriminate between events from incoming neutrons and events from incoming photons, a 13-cm borated paraffin absorber was placed in front of the NaI(Tl) detector in part of the experiments. For a minimum energy loss of 2 MeV, the attenuation coefficient for neutrons is a factor of 2.6 larger than the attenuation coefficient of 17.64-MeV photons. Therefore, a background produced by neutrons should become visible when measuring with and without the borated paraffin absorber. None of the results obtained with the absorber showed a difference compared to measurements without the absorber. For the same reason and to safely discriminate between elastic and Raman scattering, a Ge(Li) detector instead of a NaI(Tl) detector has been used for the 17.64-MeV data point of ^{238}U.

For the experiment at the BR2 reactor, Ge(Li) detectors were used in all cases. Therefore, the background produced by neutrons was not a problem. In order to avoid damage of the Ge(Li) detectors, neutrons leaving the reactor were filtered out of the beam by 45 cm of borated polyethylen. Photoneutrons produced in the
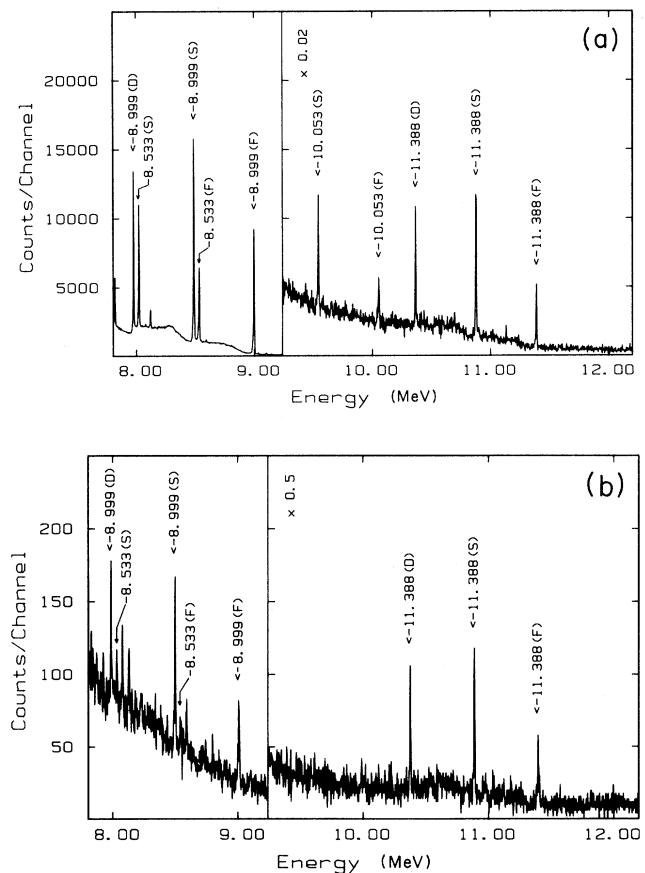
from the source. It should be noted that a large range of scattering angles may be tolerated in a large-angle photon scattering experiment without any loss in accuracy. This is due to the fact that the angular dependence of the elastic differential cross section is a slowly varying function without any structure. Therefore, a firm relation is given between the average over a larger interval and the differential cross section at a specific angle.

The energy-proportional pulses of the Ge(Li) or NaI(Tl) detectors were analyzed by an analog-to-digital converter (ADC). The time signals of these detectors were used to start, and the signal of the plastic veto counter to stop a time-to-amplitude converter (TAC). Using single-channel analyzers (SCA), two windows were set upon the TAC spectrum, one for the true-plus-random, the other for random events. The output events of the SCA's were used for routing the energy spectra into quarters of a 4096 channel memory. Events N_A not being in coincidence with any of the SCA's are due to scattering, with the count rate slightly reduced by random coincidence losses N_r, as routed by the second SCA. Then the corrected spectrum of scattered photons was given by $N_{AK}=N_A+2N_r$.

Care had to be taken because of photoneutrons produced in the scattering target, the rate of which being roughly 100 times the rate of elastically scattered photons. When using a Ge(Li) detector the possible damage is the only problem. In case of NaI(Tl) detectors, neutrons may contribute to the background underneath the elastic line. This may occur[18] when the neutron binding energies in ^{24}Na (6959 keV) and ^{128}I (6826 keV) are not smaller than the binding energies in the scattering materials under investigation[19] (^{181}Ta: 7644 keV; ^{203}Tl: 7720 keV; ^{205}Tl: 7541 keV; ^{209}Bi 7453 keV; ^{238}U: 6144 keV) by at least the width of the response function of the

FIG. 3. Photon spectra provided by the ^{58,59}Ni(n,γ) reaction and registered by a Ge(Li) detector. (a) Direct spectrum. (b) Spectrum of photons scattered by Tl through $\theta=136°$.

scattering target were absorbed in 15 cm of borated paraffin positioned in front of the detector.

Typical spectra obtained in the present work are depicted in Figs. 3–5. Figure 3(a) shows the direct spectrum measured at the BR2 reactor, Fig. 3(b) the correspo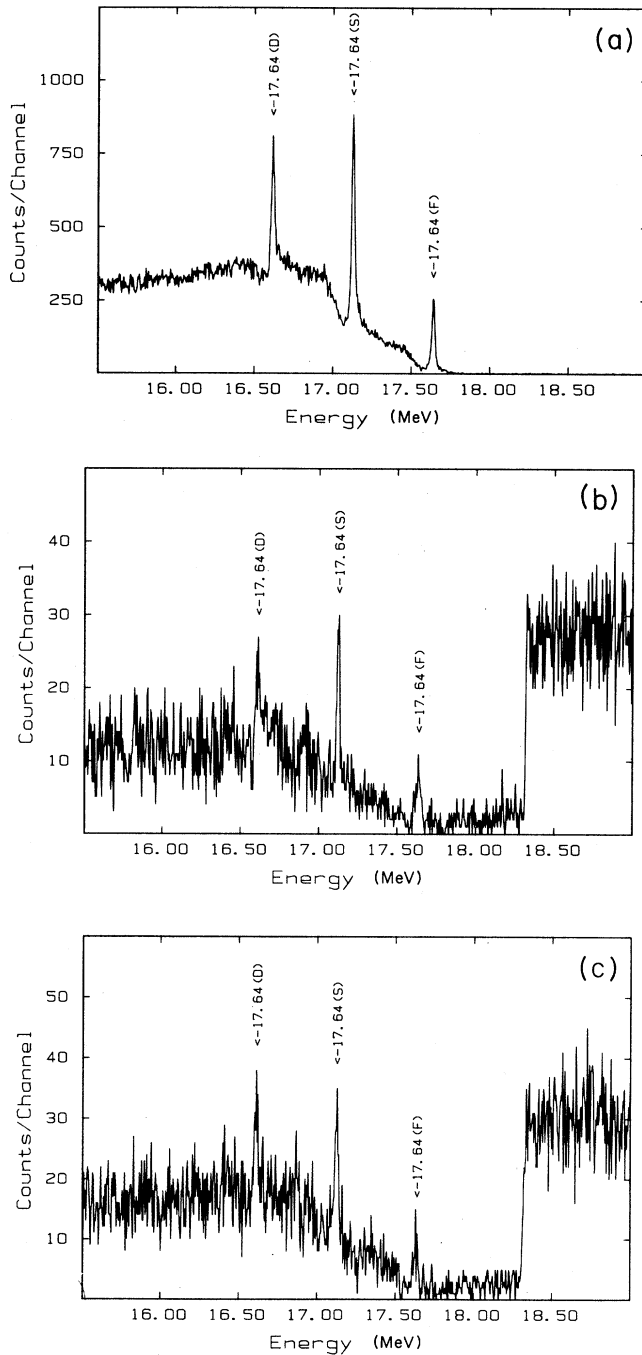nding spectrum of photons scattered by Tl. It should be emphasized that due to the background suppression by the plastic-scintillator anticoincidence shield, the line of elastically scattered photons is on top of only a comparatively low background. Figure 4(a) shows the direct spectrum measured with photons from the ^{7}Li(p,γ) reaction, Figs. 4(b) and 4(c) the corresponding spectra of photons scattered by ^{209}Bi and ^{238}U, respectively. In order to demonstrate the large importance of the anticoincidence shield, the spectra of Figs. 4(b) and 4(c) also contain that portion above 18.3 MeV where due to the window settings of the electronics the anticoincidence shield is not effective. This use of a muon shield in connection with a Ge(Li) detector is a new development which apparently is capable of reducing the background drastically. Figure 5 shows spectra of photons measured with the 17.64-MeV photon beam using a 16 cm×16 cm×24 cm NaI(Tl) detector. The upper part of this figure depicts the direct beam, the lower part of the spectrum of photons scat-

FIG. 4. Photon spectra provided by the ^{7}Li(p,γ) reaction and registered by a Ge(Li) detector. (a) Direct spectrum. (b) Scattered by ^{209}Bi through $\theta=98°$. (c) Scattered by ^{238}U through $\theta=92°$.
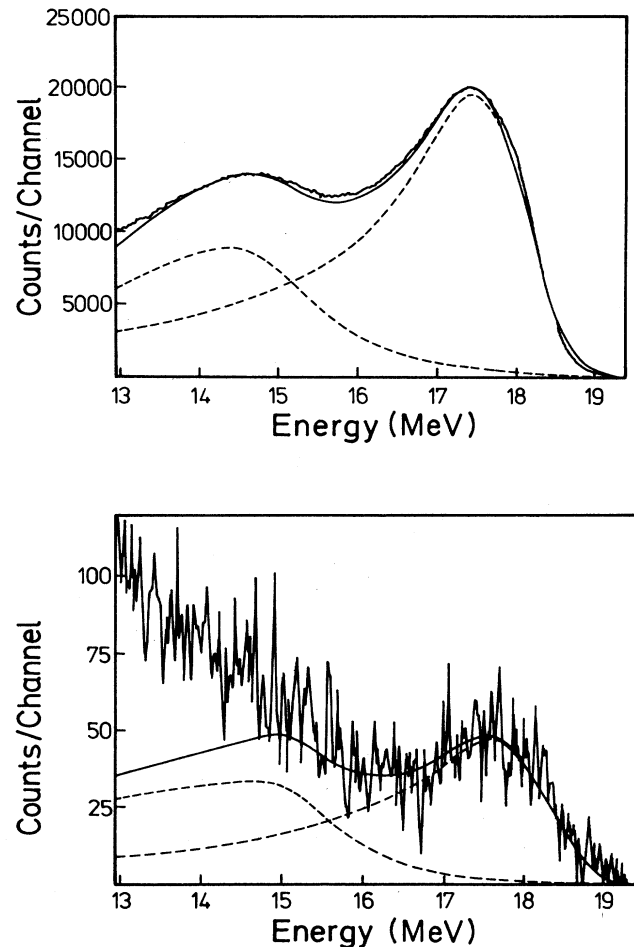
FIG. 5. Spectra of photons from the ^{7}Li(p,γ) reaction measured with a 16×16×24 cm^3 NaI(Tl) detector. Upper part: Direct spectrum. Lower part: Spectrum of photons scattered by ^{209}Bi through $\theta=95°$. Dashed curves: Partial spectra of the 17.64- and 14.7-MeV lines. Solid curves: Sum of partial spectra.

TABLE I. Differential cross section for quasielastic photon scattering by ^{181}Ta measured with a NaI(Tl) detector.

E_γ (MeV)	θ	$\left[\dfrac{d\sigma}{d\Omega}\right]_{exp}$ $\left[\dfrac{\mu b}{sr}\right]$
17.64	62°	392 (25)[a]
	95°	345 (25)[a]
	137°	464 (28)[a]

[a]The present work.

TABLE III. Differential cross sections for elastic photon scattering by ^{209}Bi.

E_γ (MeV)	θ	$\left[\dfrac{d\sigma}{d\Omega}\right]_{exp}$ $\left[\dfrac{\mu b}{sr}\right]$
8.999	60°	29.0 (4.3)[a]
	90°	13.0 (1.9)[a]
	120°	9.6 (1.3)[a]
	135°	14.0 (3.0)[b]
9.720	60°	39.0 (13.0)[a]
	90°	23.7 (4.8)[a]
	120°	14.0 (4.2)[a]
11.388	60°	375 (147)[a]
	120°	189 (47)[a]
	135°	240 (48)[b]
17.64	72°	394 (24)[c]
	95°	364 (32)[c]
	98°	344 (21)[b]
	134°	522 (32)[c]

[a]Measured with a Ge(Li) detector, our previous work (Ref. 21).
[b]Measured with a Ge(Li) detector, the present work.
[c]Measured with a NaI(Tl) detector, the present work.

tered by ^{209}Bi through $\theta = 95°$. The direct spectrum has to be decomposed into two parts, corresponding to the 17.64- and 14.7-MeV lines. This can easily be achieved by making use of the known peak positions, natural widths (10.7 keV and 1.45 MeV, respectively), and intensity ratio [I (14.7 MeV)/I (17.64 MeV) = 1:2.0 (3)] of the lines. In case of the 17.64-MeV line the natural width is much smaller than the detector response function, whereas in case of the 14.7-MeV line both parts are comparable. Therefore, the detector-response function was taken from the 17.64-MeV line and folded into the natural line shape of the 14.7-MeV γ transition. For this procedure, the response function of the NaI(Tl) detector has been calculated by a Monte Carlo program.[20] With the result of this calculation, a good fit to the empirical detector-response function was obtained, after some minor modifications of the calculated response function had been carried out. With the shapes of the two lines, the spectrum of scattered photons was disentangled by the same procedure as used for the direct beam, with the only difference that the intensity ratio of the two lines had to be corrected for differences in the elastic differential cross sections at the two energies. For this correction the predicted ratio of elastic differential cross sections was of sufficient accuracy.

For the determination of the experimental elastic differential cross section only the ratio of intensities in the direct and scattered spectra has to be known. Apparently, in both spectra of Fig. 5 there is a broad range of energies between 17 and 19 MeV where the background from the 14.7-MeV line underneath the 17.6-MeV line is small and, therefore, a precise determination of the intensity ratio is possible. The uncertainty in the intensity ratio due to the 14.7-MeV line amounts to about 2%. The elastic differential cross section measured in the

$A = 181$ to 238 mass range are listed in Tables I–IV together with data of our previous investigation.[21] Because of the much larger detection efficiency of the detector, experiments with a NaI(Tl) detector are much easier to perform than experiments with a Ge(Li) detector. As an example, the scattering experiments of the ^{238}U and ^{209}Bi scattering targets carried out at 17.64 MeV using a Ge(Li) detector took 150 h of beam time, whereas with a NaI(Tl) detector the beam time was only about 30 h. Therefore, in spite of the disadvantage in energy resolution, the NaI(Tl) detector was used for part of the experiments. In Tables I–IV experiments carried out with the NaI(Tl) detector are named quasielastic, because possibly existing transitions to low-lying excited states are not resolved from the elastic transition.

III. THEORY

A. The amplitude for coherent elastic scattering

In the energy range of interest to this work the amplitude for coherent elastic scattering is given by

TABLE II. Differential cross section for elastic scattering of photons by ^{nat}Tl measured with a Ge(Li) detector.

E_γ (MeV)	θ	$\left[\dfrac{d\sigma}{d\Omega}\right]_{exp}$ $\left[\dfrac{\mu b}{sr}\right]$
8.533	136°	5.0 (3.0)[a]
8.999	136°	14.5 (2.5)[a]
11.388	136°	200 (28)[a]
17.64	134°	433 (28)[a]

[a]The present work.

TABLE IV. Differential cross sections for elastic photon scattering by ^{238}U measured with a Ge(Li) detector.

E_γ (MeV)	θ	$\left[\dfrac{d\sigma}{d\Omega}\right]_{exp}$ $\left[\dfrac{\mu b}{sr}\right]$
8.533	90°	17 (9)[a]
8.884	90°	25 (6)[a]
8.998	60°	36 (8)[a]
	90°	30 (3)[a]
9.720	60°	61 (23)[a]
	90°	73 (11)[a]
17.64	90°	320 (40)[b]

[a]Our previous work (Ref. 21).
[b]The present work.

$$f_{\text{tot}}(E,\theta)=f_A(E,\theta)+f_D(E,\theta) \ , \tag{1}$$

where f_A stands for the nuclear scattering amplitude and f_D for the Delbrück (D) amplitude. In addition to the energy E and the scattering angle θ, the scattering amplitudes depend also on the polarization of the photon.

B. Nuclear coherent elastic (Compton) scattering

According to our present understanding the nuclear coherent elastic (Compton) amplitude may be written in the form[9,22−24]

$$f_A(E,\theta)=B(E,\theta)+T(E,\theta)+S(E,\theta) \ , \tag{2}$$

where $B(E,\theta)$ corresponds to the kinetic seagull term, $T(E,\theta)$ to scattering through nuclear resonant (NR) and quasideuteron (QD) excited states including the dipole spurious motion of the nucleus, and $S(E,\theta)$ to scattering through the mesonic seagull and mesonic intermediate states. In principle, the excitation of internal degrees of freedom of the nucleons also has to be taken into account which, however, at these low energies may safely be disregarded. The first term in (2) is the scattering by Z independent protons and may be calculated from the charge form factor $F_p(q)$ of the nucleus

$$B(E,\theta)=-\frac{Ze^2}{Mc^2}\boldsymbol{\varepsilon}'\cdot\boldsymbol{\varepsilon}F_p(q) \ , \tag{3}$$

where $\boldsymbol{\varepsilon}$ and $\boldsymbol{\varepsilon}'$ are the polarization vectors of the incoming and outgoing photon, respectively. The quantity $T(E,\theta)$ may be represented in the form

$$
\begin{aligned}
T(E,\theta)=\ &R_{E1}(E)\boldsymbol{\varepsilon}'\cdot\boldsymbol{\varepsilon}+R_{E2}(E)g_{E2}\\
&+R_{\text{QD}}(E)\boldsymbol{\varepsilon}'\cdot\boldsymbol{\varepsilon}F_{\text{ex}}(q)\\
&+\frac{NZ}{AMc^2}e^2[1+\kappa_{\text{GDR}}+\kappa_{\text{QD}}F_{\text{ex}}(q)]\boldsymbol{\varepsilon}'\cdot\boldsymbol{\varepsilon} \ ,
\end{aligned}
\tag{4}
$$

where the $E2$ angular distribution function is given by

$$g_{E2}=2(\boldsymbol{\varepsilon}'\cdot\boldsymbol{\varepsilon})(\hat{\mathbf{k}}'\cdot\hat{\mathbf{k}})-(\boldsymbol{\varepsilon}'\times\hat{\mathbf{k}}')\cdot(\boldsymbol{\varepsilon}\times\hat{\mathbf{k}}) \tag{5}$$

and κ_{GDR} and κ_{QD} are the dipole enhancement factors for the GDR and QD energy ranges, respectively. The QD part of (4) is multiplied by a form factor, because for this mode of nuclear excitation the different volume elements may be considered as independent radiators. The quantities $R(E)$ in (4) are obtained by applying the once subtracted dispersion relation

$$
\begin{aligned}
\text{Re}R(E)&=\text{Re}T(E,0)-T(0,0)\\
&=\frac{E^2}{2\pi^2\hbar c}P\int_0^\infty\frac{\sigma(E')}{E'^2-E^2}dE'
\end{aligned}
\tag{6}
$$

and optical theorem

$$\text{Im}R(E)=\frac{E}{4\pi\hbar c}\sigma(E) \tag{7}$$

to the total nuclear photoabsorption cross section. It is easy to see that the form of $T(E,\theta)$ as given in (4) is chosen such that the electric dipole parts vanish in the limit $E\rightarrow\infty$ for all angles θ, whereas the electric quadru-

pole part is treated as a small correction, as it really is.

The quantity $S(E,\theta)$ is given by

$$S(E,\theta)=-\frac{NZ}{AMc^2}e^2(\kappa_{\text{GDR}}+\kappa_{\text{QD}})\times F_{\text{ex}}(q)\boldsymbol{\varepsilon}'\cdot\boldsymbol{\varepsilon} \ . \tag{8}$$

The form factor in (8) is suggested by the fact that the largest part of $S(E,\theta)$ is believed to be due to the mesonic seagull term.[9,22−24] $S(E,\theta)$ cancels the κ-dependent parts in (4) in the forward direction and restores the classical Thomson formula for $f_A(E,\theta)$ in the limit $E\rightarrow0$. Summarizing, we can represent $f_A(E,\theta)$ as a sum of the first three terms in (4) and modified Thomson (MT) amplitude (nonresonant exchange term[25])

$$
\begin{aligned}
f_{\text{MT}}(E,\theta)=-\frac{e^2}{Mc^2}\bigg[&ZF_p(q)-\frac{NZ}{A}(1+\kappa_{\text{GDR}})\\
&+\frac{NZ}{A}\kappa_{\text{GDR}}F_{\text{ex}}(q)\bigg]\boldsymbol{\varepsilon}\cdot\boldsymbol{\varepsilon}' \ .
\end{aligned}
\tag{9}
$$

The exchange form factor $F_{\text{ex}}(q)$ introduced in (4) corresponds to the spatial distribution of correlated proton-neutron pairs. The rms radius describing the spatial distribution of these pairs may possibly be smaller than the rms charge radius. However, in the GDR region the modification of the total amplitude $f_A(E,\theta)$ due to form factors is not larger than 5%. Therefore, the possible deviation of $F_{\text{ex}}(q)$ from $F_p(q)$ may safely be disregarded.

It should be noted that in the framework of the present treatment only the resonant part of the enhancement factor, viz. κ_{GDR}, enters into the modified form factor. This important point has been stated for the first time by Ziegler.[25] It was the purpose of the discussion given above to make the premises entering into the modified form factor transparent. If the GDR photoabsorption cross section is given by a superposition of Lorentzian lines, the amplitudes defined in (6) and (7) are given by

$$
\begin{aligned}
R_{E1}(E)&=\sum_{j=1}^2(\alpha_j+i\beta_j)\\
&=\frac{E^2}{4\pi\hbar c}\sum_{j=1}^2\sigma_j\Gamma_j\frac{E_j^2-E^2+i\Gamma_jE}{(E_j^2-E^2)^2+\Gamma_j^2E^2} \ .
\end{aligned}
\tag{10}
$$

In the energy range of interest, scattering through QD excitation modifies the elastic differential cross section by only a few percent. The necessary correction is calculated by applying the optical theorem and the dispersion relation to Levingers modified QD formula

$$\sigma_{\text{QD}}(E)=L\frac{NZ}{A}\exp\left[-\frac{D}{E}\right]\sigma_D(E) \tag{11}$$

with $L=8$, $D=60$ MeV, and $\sigma_D(E)$ the deuteron photoabsorption cross section.

C. Nuclear Raman scattering

The coupling of the GDR vibration to the nuclear surface has two observable effects: (i) there is a broadening of the photoabsorption cross section and (ii) electromagnetic transitions become possible to collective rotational

and surface-vibrational states. This latter phenomenon is termed nuclear Raman scattering.

Rotational nuclei may be described by the modified simple rotator model (MSRM). Using the two-Lorentzian representation of (10) for the GDR photoabsorption cross section, the differential cross section for Raman scattering is given by

$$\left[\frac{d\sigma}{d\Omega}\right]_R = (I_0 K_0 20 | I_f K_0)^2$$

$$\times [(2\alpha_1 - \alpha_2)^2 + (2\beta_1 - \beta_2)^2]\frac{13 + \cos^2\theta}{40} ,$$

$$\text{(12)}$$

where the Clebsch-Gordan coefficient depends on the spins of the initial and final states. To our present knowledge[26,21] good rotators are well described by the MSRM provided the GDR parameters are of sufficient accuracy.

Our knowledge of Raman transitions into vibrational modes is less certain.[27] The dynamic collective model (DCM) which has been developed to describe the coupling between GDR and surface vibration predicts a substantial photon decay branch to the $K=2,2^+$ γ-vibrational bandhead of axially-symmetric deformed even-even nuclei. Qualitatively, the same result is obtained on the basis of the interacting boson model (IBM).[28,29] A difference between the two models is that for the IBM the surface modes are less collective than for the DCM and, therefore, the predicted branchings are smaller.[28]

D. Delbrück scattering

The most recent investigation of Delbrück (D) scattering has been carried out by Rullhusen et al.[30]. Two approaches are compared with each other. The first makes use of the lowest-order Feynman graphs (LOF) and allows an exact calculation of the imaginary as well as the real D amplitude to this order but ignores the Coulomb correction effect. The second uses the impact-factor method (IFM) which takes into account the Coulomb correction effect but ignores the real D amplitude. Both predictions are shown[30] to be in agreement with the scaling laws of Cheng, Tsai, and Zhu,[31] predicting that for fixed angle θ the amplitude scales in the form $\omega^{1-} f(\theta)$ as $\omega/m \rightarrow \infty$, where ω is the photon energy and m the electron mass. This scaling law was shown[30] to be very useful for the interpolation between inaccurate or incomplete D amplitudes and for extrapolating them to high energies. The IFM is a high-energy small-angle approximation which grossly fails at the scattering angles and energies investigated in the present experiment. Therefore, only LOF predictions are available for the interpretation of the present experimental data, supplemented by some semi-empirical corrections[21] taking into account the Coulomb correction effect.

The existing numerical LOF amplitudes[32,33] are very accurate in case of the imaginary parts but reveal considerable numerical inaccuracies in case of the real parts. Therefore, plots of the kind described in the paper by

Rullhusen et al.[30] have been used in order to arrive at reliable D amplitudes. Care has been taken in the use of the tabulation of Bar-Noy and Kahane[32] because different sign conventions[34] are used for the real and imaginary parts.

Previous elastic photon scattering experiments[21] carried out in the 8.5–11.4 MeV energy range and 181–238 mass range led to the definite conclusion that the Coulomb correction effect is quite important. By a careful comparison of predicted and measured scattering amplitudes it was possible to arrive at an empirical ansatz for the Coulomb correction term, viz.

$$C(E,\theta) = (Z\alpha)^4 g(E)f(\theta) \times 10^{-3} r_0 \tag{13}$$

with

$$g_\parallel(E) = g_\perp(E) = 15 - \tfrac{1}{9}(E+6)^2 , \tag{14}$$

and

$$f_\parallel(\theta) = 1 + 0.47(X-1) , \tag{15}$$

$$f_\perp(\theta) = 1 - 0.33(X-1) , \tag{16}$$

where E (MeV) is the photon energy, $X = \sin^{-2}(\theta/2)$, and r_0 the classical electron radius. In arriving at the Coulomb correction term given above use has been made of the assumption[21] that $\text{Re}C_\parallel = \text{Im}C_\parallel$ and $\text{Re}C_\perp = \text{Im}C_\perp$. These assumptions are suggested by the fact that analogous relations are approximately valid for the lowest-order amplitudes.

The Coulomb correction terms of (13)–(16) are valid only in the 8 to 12 MeV energy range. Therefore, at higher energies only the lowest-order amplitudes are available. This, however, is not a serious drawback because at these higher energies the contribution of D scattering to the total amplitudes becomes small at large angles.

IV. RESULTS

In the following we use the experimental elastic differential cross section determined in the present investigation for an improvement on GDR parameters. This will be carried out by comparing the experimental data with predictions including the GDR, Delbrück (D) scattering in lowest order, the semi-empirical corrections for the Coulomb correction effect, the isovector giant-quadrupole resonance (GQR), and the quasideuteron (QD) effect.

A. Tantalum

Figure 6 shows the quasielastic differential cross sections measured for ^{181}Ta at 17.64 MeV together with predictions, calculated using the GDR parameters of Table V. The set of GDR parameters underlying curve 1 were extracted by Bar-Noy and Moreh[35] from the photoabsorption data of the Saclay[36] and Melbourne[37] groups and modified to fit their[36] photon scattering data in the 8.5–11.4 MeV range. The good fit in the 8.5–11.4 MeV range has been confirmed in our previous study[21] whereas in Fig. 6 curve 1 reveals a deviation from the 17.64-MeV experimental data. The original GDR parameters from

TABLE V. Lorentz parameters for the GDR of ^{181}Ta used for the calculations in Fig. 6. $R = (\sigma_1\Gamma_2)/(\sigma_1,\Gamma_1)$, the ratio of areas underneath the Lorentzians, Σ_{GDR}, the sum of areas underneath the Lorentzians in units of the TRK sum rule.

Curve	E_i (MeV)	σ_i (mb)	Γ_i (MeV)	R	Σ_{GDR}	Reference
1	12.49	253	2.62	1.95	1.18	35
	15.38	302	4.29			
2	12.35	270	2.57	2.12	1.30	36
	15.30	330	4.47			
3	12.50	255	2.23	2.16	1.08	37
	15.41	308	3.98			
4	12.49	247	2.62	2.19	1.24	The present work
	15.38	330	4.29			

photoneutron work[36,37] are used for the calculation of curves 2 and 3, respectively. The best overall fit to all the existing photon scattering data in the 8.5–11.4 MeV range as well as at 17.64 MeV (curve 4 in Fig. 6) was obtained by using the GDR parameters of Bar-Noy and Moreh[35] after a small shift in the peak cross sections, i.e., decreasing σ_1 by 2% and increasing σ_2 by 9% (parameters of curve 4 in Table V).

B. Thallium

Data on the GDR of the Tl isotopes are very scarce. There are no accurate photoneutron data available.
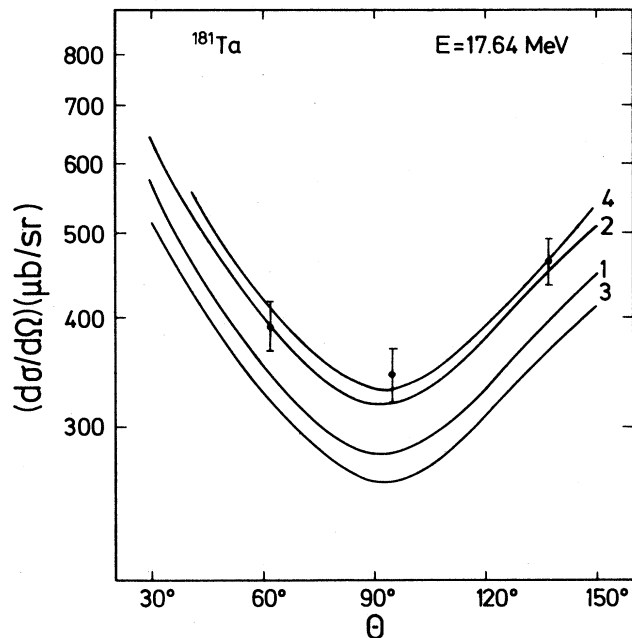

FIG. 6. Differential cross section for quasielastic scattering of 17.64-MeV photons by ^{181}Ta vs scattering angle measured with a $16 \times 16 \times 24$ cm^3 NaI(Tl) detector. Curves: Predictions including elastic photon scattering and a small correction (15 μb/sr) for incoherent scattering according to the modified simple rotator model (MSRM). The different GDR parameters are listed in Table V.

Laszewski and Axel[38] have measured photon scattering below the particle threshold and have used GDR parameters extracted from the data of Antropov et al.[39]. These parameters are listed in Table VI and are used to calculate the curve (1) of Fig. 7. Apparently, there is a large discrepancy between the prediction based on these[38,39] GDR parameters and our experimental data, mainly because of the peak cross section σ_0. Since no good photoneutron data are available for Tl, our improvement procedure to some extent also includes the peak energy E_0 and the width Γ of the GDR. The set of GDR parameters used for the calculation of curve (2) in Fig. 7 are the result of a least-squares fit to our experimental elastic differential cross sections. They are listed in Table VI and correspond to $\Sigma_{GDR} = 1.37$ TRK sum rules. This value has to be compared with $\Sigma_{GDR} = 0.97$ TRK sum-rule units calculated from the parameter set of curve 1.

C. Bismuth and lead

The GDR of ^{209}Bi has previously been investigated via elastic photon scattering by the present authors.[13,21] In the present work this nucleus has been used to test the consistency of elastic differential cross sections previously measured at the Grenobel reactor[21] and presently measured at the Mol reactor. As is demonstrated in Fig. 8 there is a very close agreement between the two sets of data, confirming their expected good precision. A comparison between experiment and predictions based on different sets of GDR parameters as listed in Table VII is carried out in Figs. 9 and 10. The best overall agreement is with curves 1 obtained by using the Livermore GDR parameters[40] with the peak cross section multiplied by 1.35. This agreement between experiment and curves 1 confirms the rather large integrated cross section of $\Sigma_{GDR} = 1.46$ TRK sum rules underneath the Lorentzian.[13] It should be noted that the data analysis of Ref. 13

TABLE VI. Lorentz parameters for the GDR of ^{nat}Tl used for the predicted curves in Fig. 7. Meaning of R and Σ_{GDR} same as in Table V.

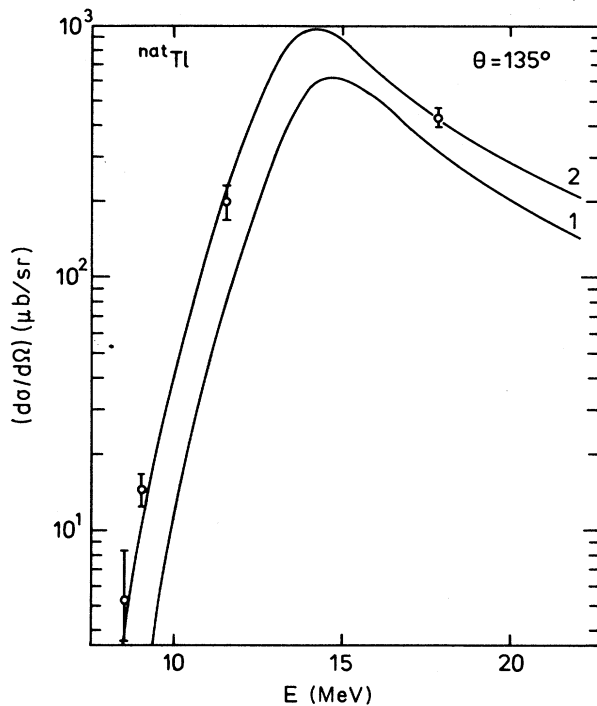| Curve	E_0 (MeV)	σ_0 (mb)	Γ_0 (MeV)	Σ_{GDR}	Reference
1	14.1	490	3.7	0.97	38
2	13.3	640	4.0	1.37	The present work

FIG. 7. Differential cross section for elastic scattering of 8.5–18-MeV photons by Tl vs energy, measured with a Ge(Li) detector. The curves have been calculated using the GDR parameters of Table VI.

FIG. 9. Differential cross sections for elastic scattering of 17.64-MeV photons by ^{209}Bi vs scattering angle. Closed circles: measured with a $16 \times 16 \times 24$ cm^3 NaI(Tl) detector. Open circle: measured with a Ge(Li) detector (data from present work).

includes also the quasideuteron (QD) effect, using the same procedure as used in the present paper. This fact has not been mentioned explicitly in Ref. 13 because the influence of the QD effect on the GDR parameters extracted from the elastic differential cross sections is small.

Based on only the data points below 12 MeV, Kahane[34] arrives at a somewhat (8%) smaller peak cross section by
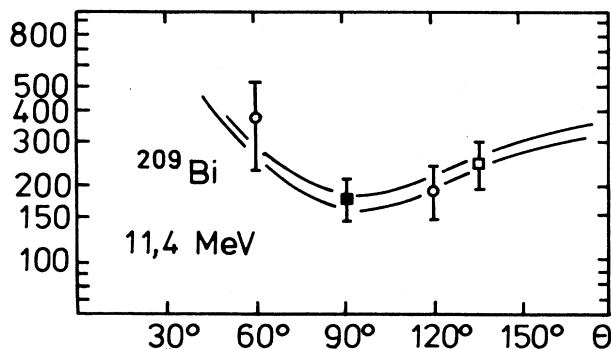

FIG. 8. Differential cross section for elastic scattering of 11.4-MeV photons by ^{209}Bi vs scattering angle. Open circles: measured by the present authors at the Grenoble high-flux reactor (Ref. 21). Open square: measured at the Mol reactor (present work). Closed square: interpolated along the curves. The curves are identical to curves (a) and (d) in Fig. 10 of Ref. 21.
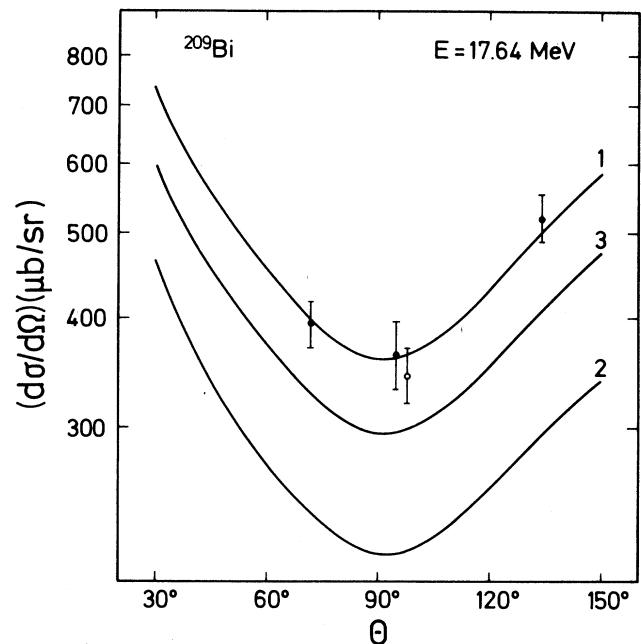
using a spline fit to the experimental photoneutron data[40] instead of a Lorentzian fit. Figure 11 shows an extension of Kahane's procedure to higher energies when raising the photoneutron data of the Livermore group by a factor of 1.24 instead of our factor of 1.35. The factor of 1.24 is suggested by the Illinois experiment[41] and has been favored by Kahane.[34] Apparently, there is no fit to the experimental elastic differential cross section at 17.64 MeV though the spline procedure produces a local maximum at this energy. Furthermore, by inspecting the photoneutron data, it appeared to us likely that the structures in the photoabsorption cross section might be due to statistical fluctuations in a first place. This supposition is strongly supported by the following considerations. Elastic photon scattering experiments carried out[42] on ^{208}Pb in the energy range between 9.5 and 12 MeV showed a remarkable structure in case of ^{208}Pb whereas the differential cross section of ^{206}Pb was completely smooth. This finding is explained by Fig. 12, showing the level spacings[43] of ^{208}Pb, ^{206}Pb, and ^{209}Bi as a function of energy. The level spacings of ^{208}Pb are two orders of magnitude larger than those of ^{206}Pb. If we now realize that the level spacings of ^{209}Bi are three orders of magnitude smaller than those of ^{208}Pb, structures in the photoabsorption cross section of ^{209}Bi appear to be very unlikely.

After this work has been completed the GDR of ^{209}Bi has been reinvestigated[44] in the 12–18 MeV energy range using tagged photons. This investigation[44] confirms our rather large peak cross section of $\sigma_0 = 703$ mb within 1% but arrives at a 14% smaller width Γ. We have com-
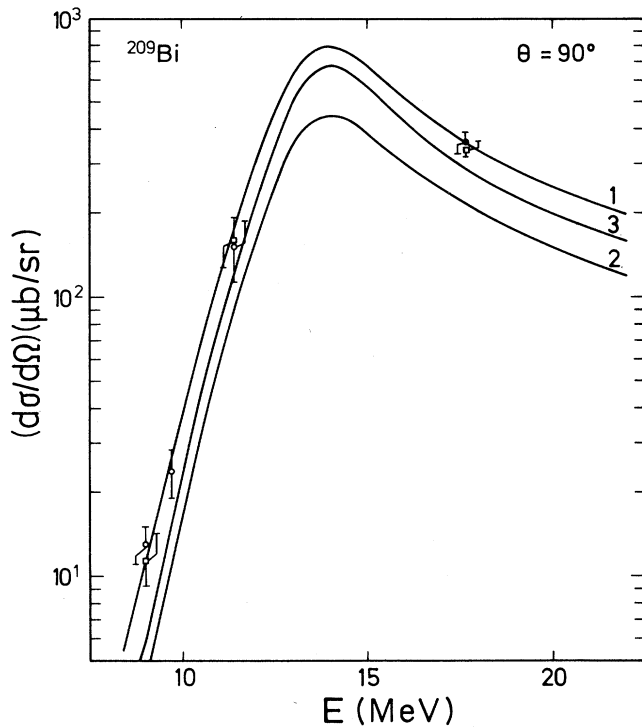
FIG. 10. Differential cross sections for elastic scattering of photons by ^{209}Bi through $\theta = 90°$ vs energy. Open squares: measured with a Ge(Li) detector (present work). Open circles: measured with a Ge(Li) detector at the Grenoble reactor (Ref. 21). Closed circles: measured with a $16 \times 16 \times 24$ cm^3 NaI(Tl) detector (present work). Curves: calculated using the Lorentz parameters of Table VII. The data at 11.4 MeV (open circle, open square) and 8.999 MeV (open square) are calculated from data measured at 120° and 135°.

pared the GDR parameters of Ref. 44 with our photon scattering data at 17.64, 11.4, and 9.0 MeV and with the photoabsorption data of Refs. 40 and Ref. 41. This comparison showed that the smaller width Γ of Ref. 44 is inconsistent with all three sets of data whereas our larger width is consistent. Details of this investigation will be published in a forthcoming paper. This experience with data from tagged photon experiments makes us also hesitate to include the ^{206}Pb data of Ref. 15 into the present discussion, hoping that the discrepancy found in case of ^{209}Bi may be cleared up in future experiments.

We did not apply our method of peak cross section scaling to ^{208}Pb because of the structures in the GDR

TABLE VII. Lorentz parameters for the GDR of ^{209}Bi used for the predicted curves in Figs. 9 and 10. The meaning of R and Σ_{GDR} are the same as in Table V.

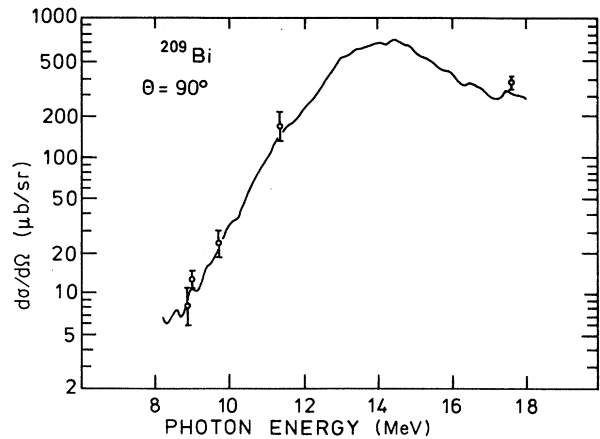| Curve	E_0 (MeV)	σ_0 (mb)	Γ_0 (MeV)	Σ_{GDR}	Reference
1	13.45	703	3.97	1.46	21
2	13.45	521	3.97	1.08	40
3	13.56	648	3.72	1.26	41

FIG. 11. Same as Fig. 10, but compared with a prediction obtained by the method proposed by Kahane (Ref. 34), using a scaling factor of 1.24 to increase the Livermore (Ref. 40) photoneutron cross sections.
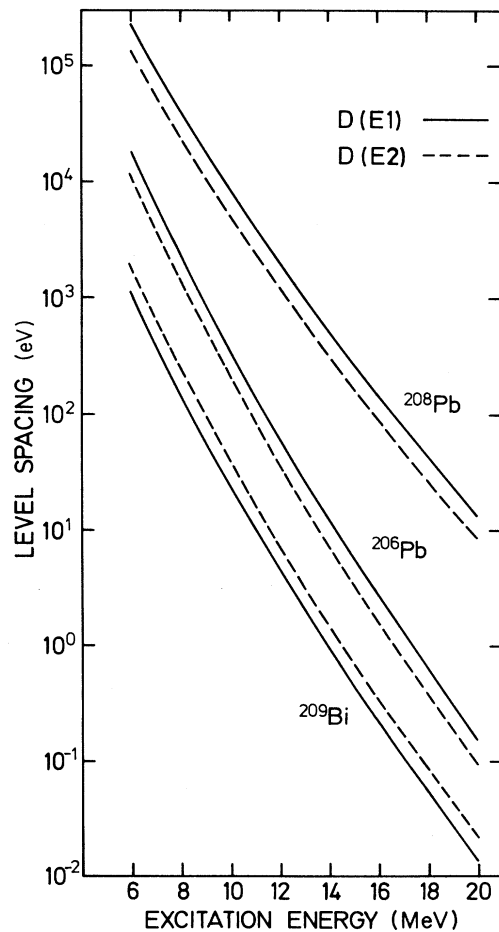

FIG. 12. Predicted (Ref. 43) level spacings for electric dipole ($E1$) and electric quadrupole ($E2$) excitation vs energy.

TABLE VIII. Lorentz parameters for the GDR of ^{238}U used for the predicted curves in Fig. 13. The meanings of R and Σ_{GDR} are the same as in Table V.

Curve	E_i (MeV)	σ_0 (mb)	Γ_i (MeV)	R	Σ_{GDR}	Reference
1	10.96	301	2.90			
	14.04	369	4.53	1.92	1.18	47
2	10.96	319	2.90			
	14.04	391	4.53	1.92	1.25	21
3	10.77	311	2.37			
	13.80	459	5.13	3.19	1.43	48

photoabsorption cross section of this nucleus. There are, however, photon scattering data obtained by using photons from positron annihilation in flight.[45] The way of partitioning the photoabsorption cross section into a GDR and a QD part, however, is different from that used in the present paper, making a comparison difficult. Instead we use the GDR parameter of Veyssière et al.[46] and Berman et al.[16] for the discussion given in Sec. V.

D. Uranium and thorium

The GDR of ^{238}U has previously been investigated via elastic and Raman scattering carried out in the 8–12 MeV energy range.[21] The GDR parameters determined in this way are listed in Table VIII, together with the GDR parameters from photoneutron measurements of
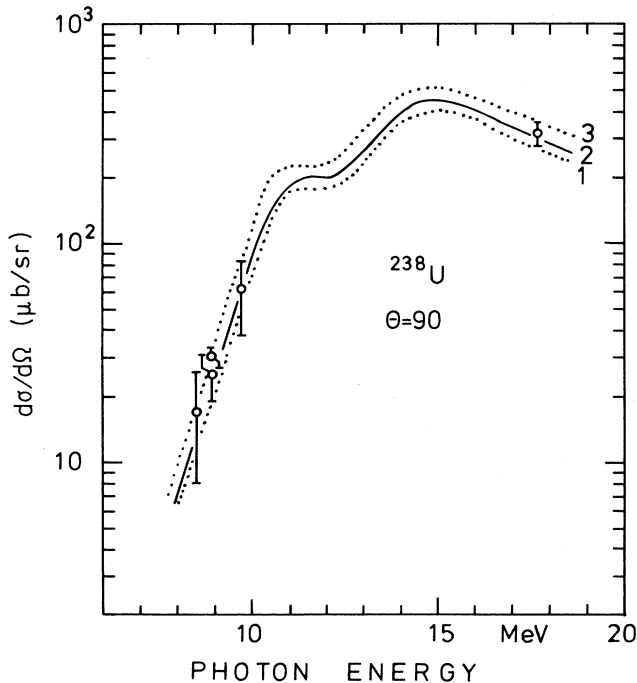

FIG. 13. Differential cross section for elastic scattering of photons by ^{238}U through $\theta = 90°$ vs energy. Data from our present and previous (Ref. 21) works. Curve 1: calculated using the Saclay (Ref. 47) GDR parameters. Curve 2: calculated using the GDR parameters of our previous work (Ref. 21). Curve 3: calculated using the Livermore (Ref. 48) GDR parameters.

the Saclay[47] and Livermore[48] groups. We[21] have based our scaling procedure on the peak energies E_i the widths Γ_i and intensity ratio $R = (\sigma_2\Gamma_2)/(\sigma_1\Gamma_1)$ of the Saclay[47] data because the experimental cross sections of rotational Raman scattering are in favor of these data.[21] This is not surprising, because the intensity ratio R of the Livermore[48] GDR parameters amounts to $R = 3.2$ which is quite unusual. A good fit to the elastic differential cross sections in the 8–12 MeV range was obtained by using the Saclay GDR parameters, but increasing both peak cross sections by a factor of 1.06. This previous finding is confirmed in Fig. 13 where the differential cross section measured in the present work at 17.64 MeV using a Ge(Li) detector is in favor of curve 2, though the deviations of curves 1 and 3 from the data amounts to only one standard deviation. From this observation we may conclude that our method of shifting both peak cross sections of the Saclay[47] GDR parameters by the same factor is correct. It should be noted that Fig. 13 contains only a small fraction of the data available in the 8–12 MeV range and that the scaling procedure applied in Ref. 21 were based on all the data available in this energy range. For ^{238}Th the findings[21] were analogous to those for ^{238}U. Therefore, we did not reinvestigate this nucleus. Instead we used our previously determined GDR parameters for the determination of κ_{GDR}.

V. DISCUSSION

According to the tables presented in Sec. IV, the existing data for κ_{GDR} cover the range between 0 and 0.5 with no apparent systematics. Our intention is to arrive at a higher accuracy for κ_{GDR} in order get an information on a possibly existing systematic nuclear-structure dependence on this quantity. The procedure we apply is to compare the κ_{GDR} data from our present photon scattering investigation with κ_{GDR} data from a selected part of previous photon-absorption investigations. For this comparison we select the photon-absorption data of the Saclay group[36,46,47] and those of a recent paper by Berman et al.[16] for the following reasons: (i) The GDR parameters of the Saclay group[36,46,47] in general proved to show the best agreement with our photon scattering results wherever a comparison has been carried out and (ii) the recent data of Berman et al.[16] make use of a long experience with photoneutron measurements and, therefore, may be believed to be quite accurate.

Figure 14 shows values for κ_{GDR} selected by the criteria described above. There are three groups of data in
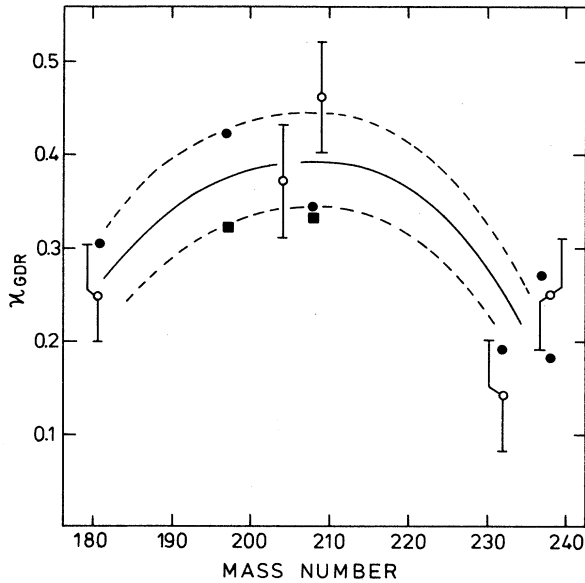
FIG. 14. Enhancement factors of the dipole strengths located in the GDR, defined via Lorentzian fits to the GDR photoabsorption cross sections. Open circles: photon scattering data of present work and Ref. 21. Solid circles: photoabsorption, Saclay (Refs. 36, 46, and 47). Solid squares: photoabsorption, Livermore (Ref. 16). Solid curve: guide for the eye, indicating a trend in the A dependence of κ_{GDR} as suggested by the data. Dashed curves: same as solid curve but shifted up or down by $\Delta\kappa_{GDR}=0.05$.

mass regions at $A=181$, 197–209, and 232–238. Within these mass regions there is agreement between the data, within the errors indicated by error bars. When attributing to all the data the same weight, the averages are $\kappa_{GDR}=0.27\pm0.05$, 0.37 ± 0.05, and 0.21 ± 0.05 for the mass regions $A=181$, 197–209, and 232–338, respectively, where $\Delta\kappa_{GDR}=0.05$ is the variance of the data. It is our belief that our method of shifting peak cross sections in order to optimize agreement with our accurate photon scattering cross section improves on the accuracy of the GDR parameters. Therefore, in a second approach a somewhat larger weight was given to the κ_{GDR} values obtained from photon-scattering experiments when calculating averages of κ_{GDR} in the three mass regions. The solid line is a guide for the eye drawn through these averages, thus making use of the supposition[15] that for neighboring heavy nuclei the giant-dipole resonances should be very similar. The dashed curves differ from the solid curve by adding or subtracting the variance of the data.

In the foregoing we have shown that by comparing κ_{GDR} as obtained from our photon scattering cross sections with κ_{GDR} as obtained from those selected photoneutron cross sections which we believe to be the most reliable, we arrive at a consistent information about the A dependence of κ_{GDR}. There are obvious indications in Fig. 14 that the enhancement of electric dipole strength in the GDR over the TRK sum-rule prediction is larger in the mass range around the double closed-shell nucleus

^{208}Pb as compared to open-shell nuclei. There are two possible explanations for this observation: (i) Correlation effects on the two-body force between nucleons may differ for the two types of nuclei and (ii) the clustering of dipole strength in the GDR due to residual forces[49] may be complete only for closed shells, so that for open-shell nuclei a larger fraction of the dipole strength is shifted into the high-energy tail of the GDR and, therefore, is not taken into account by the evaluation procedure applied in this paper. We tentatively assume this latter interpretation to be true. The third possibility that $E1$ strength may be shifted into the low-energy tail is ruled out by the observation[50] that for ^{239}U the low-energy tail follows the Lorentzian extrapolation of the GDR photoabsorption cross section.

It would be very interesting to have a larger number of nuclei for a comparative study of κ_{GDR}. Unfortunately, it is extremely difficult to arrive at the necessary accuracy of the data. Furthermore, for light to medium-weight nuclei the Lorentzian representation of the photoabsorption cross section is not a good approximation. This makes it impossible to use the same measure for the GDR dipole strength of different nuclei. The cutoff energy around $W_0=30$ MeV frequently used to separate the GDR and QD ranges is rather arbitrary and, therefore, introduces large uncertainties.

The appropriate tool for a microscopic investigation of giant resonances in nuclei is provided by the random phase approximation (RPA).[51] The full calculation taking into account 2p-2h configurations in addition to 1p-1h configurations can only be performed in light nuclei. For heavy closed-shell nuclei approximations such as the core-coupling RPA have been developed. This is a special type of a 2p-2h RPA which avoids the diagonalization of large matrices. The particle-hole calculations mentioned above are valid only for closed-shell nuclei. For open-shell nuclei the quasiparticle RPA has been developed, and it is an interesting question whether or not it is possible to reproduce the effect under discussion. Unfortunately, the existing calculations do not show the effect[52] and it seems to require major refinements to make these calculation sensitive to absolute values and to the detailed distribution of $E1$ strength.

Though not analogous in detail, it is interesting to know that for light nuclei the interplay between the filling of shells and the concentration or spreading of GDR $E1$ strength is a well known effect.[53,54] For the nuclei with a nearly half-filled valence shell ($A=9-11$) the valence and core nucleons contribute with comparable weight to the inclusive cross section, and the GDR, therefore, covers a broad energy region. When approaching subshell closure ($A=16$), the $E1$ strength is more and more concentrated to a narrow energy region.

VI. CONCLUSION

Though it is very difficult experimentally to arrive at a precise measure of the GDR $E1$ strength underneath the one or two Lorentzians fitting the photoabsorption cross sections of heavy nuclei, there are indications that the closure of shells leads to an increase of $E1$ strength

defined in this way. At present there is no firm interpretation of the effect. However, it appears possible that in open-shell nuclei part of the strength is shifted into the high-energy tail of the GDR and, therefore, not taken into account when defining the high-energy tail by adjusting Lorentzians to the photoabsorption cross section.

This interpretation would be in line with the observation,[55] that the $E1$ strength integrated up to pion threshold appears to be independent of the mass number A.

*Present address: Canberra Semiconductors N.V., Lammerdries 25, B-2430 Olen, Belgium.

[1]J. S. Levinger and H. A. Bethe, Phys. Rev. **78**, 115 (1950).

[2]J. Ahrens, H. Borchert, K. H. Czock, H. B. Eppler, H. Gimm, H. Gundrum, M. Kroening, P. Riehn, G. Sita Ram, A. Zieger, and B. Ziegler, Nucl. Phys. **A251**, 479 (1975).

[3]A. Leprêtre, H. Beil, R. Bergère, P. Carlos, J. Fagot, A. de Miniac, and A. Veyssière, Nucl. Phys. **A367**, 237 (1981).

[4]J. Ahrens, Nucl. Phys. **A446**, 229c (1985).

[5]A. Arima, G. E. Brown, H. Hyuga, and M. Ichimura, Nucl. Phys. **A205**, 27 (1973).

[6]W. T. Weng, T. T. S. Kuo, and G. E. Brown, Phys. Lett. **46B**, 329 (1973).

[7]M. Traini, G. Orlandini, and R. Leonardi, Riv. Nuovo Cimento **10**, 1 (1987); A. Fabrocini and S. Fantoni, Nucl. Phys. **A435**, 448 (1985) and references therein.

[8]B. R. Mottelson and S. G. Nilsson, Nucl. Phys. **13**, 281 (1959).

[9]M. Rosa-Clot and M. Ericson, Z. Phys. A **320**, 675 (1985).

[10]M. Ericson and M. Rosa-Clot, Z. Phys. A **324**, 373 (1986).

[11]J. I. Fujita and M. Ichimura, in *Mesons in Nuclei*, edited by M. Rho and D. H. Wilkinson (North-Holland, Amsterdam, 1979), Chap. 15.

[12]J. I. Fujita, S. Ishida, and M. Hirata, Supp. Prog. Theor. Phys. **60**, 73 (1976).

[13]R. Nolte, A. Baumann, K. W. Rose, and M. Schumacher, Phys. Lett. B **173**, 388 (1986).

[14]M. Schumacher, in *Capture Gamma-Ray Spectroscopy and Related Topics (Knoxville, 1984)*, Proceedings of the Fifth International Symposium on Capture Gamma-Ray Spectroscopy and Related Topics, AIP Conf. Proc. No. 125, edited by S. Raman (AIP, New York, 1984).

[15]A. M. Nathan, P. L. Cole, P. T. Debevec, S. D. Hoblit, S. F. Le Brun, and D. H. Wright, Phys. Rev. C **34**, 480 (1986).

[16]B. L. Berman, R. E. Pywell, S. S. Dietrich, M. N. Thompson, K. G. Mc Neill, and J. W. Jury, Phys. Rev. C **36**, 1286 (1987).

[17]T. Lauritzen and F. Ajzenberg-Selove, Nucl. Phys. **78**, 62 (1966).

[18]J. J. van Ruyven, Z. Sujkowski, W. H. A. Hesselink, and H. Verheul, Nucl. Instrum. Methods **216**, 141 (1983).

[19]N. B. Gove and A. H. Wapstra, Nucl. Data Tables **11**, 127 (1982).

[20]P. Corvisiero *et al.*, Nucl. Instrum Methods **185**, 291 (1981); Monte Carlo code DODIE; M. Sanzone-Arenhövel (private communication).

[21]P. Rullhusen, U. Zurmühl, F. Smend, M. Schumacher, H. G. Börner, and S. A. Kerr, Phys. Rev. C **27**, 559 (1983).

[22]H. Arenhövel, Z. Phys. A **297**, 129 (1980).

[23]P. Christillin, J. Phys. G **12**, 837 (1986).

[24]J. L. Friar and S. Fallieros, Phys. Rev. C **34**, 2029 (1986).

[25]B. Ziegler, in *New Vistas in Electro-Nuclear Physics*, edited by E. L. Tomusiak, H. S. Caplan, and E. T. Dressler (Plenum, New York, 1986), p. 293.

[26]R. Moreh, in *Intermediate Energy Nuclear Physics*, edited by R. Berger *et al.* (World Scientific, Singapore, 1982), p. 1.

[27]A. M. Nathan, Proceedings of the International Research Conference on Nuclear Structure Reactions and Symmetries, Dubrovnik, 1986 (unpublished).

[28]F. G. Scholtz and F. J. W. Hahne, Phys. Lett. **123B**, 147 (1983).

[29]G. Maino, A. Ventura, P. Van Isacker, and L. Zuffi, Phys. Rev. C **33**, 1089 (1986).

[30]P. Rullhusen, J. Trube, A. Baumann, K. W. Rose, F. Smend, and M. Schumacher, Phys. Rev. D **36**, 733 (1987).

[31]H. Cheng, E. C. Tsai, and X. Zhu, Phys. Rev. D **26**, 908 (1982).

[32]T. Bar-Noy and S. Kahane, Nucl. Phys. **A288**, 132 (1977).

[33]B. De Tollis and L. Luminari, Nuovo Cimento **81A**, 633 (1984).

[34]S. Kahane, Phys. Rev. C **33**, 1793 (1986).

[35]T. Bar-Noy and R. Moreh, Nucl. Phys. **A288**, 192 (1977).

[36]R. Bergère, H. Beil, and A. Veysière, Nucl. Phys. **A121**, 463 (1968).

[37]R. S. Hicks and B. M. Spicer, Aust. J. Phys. **26**, 585 (1973).

[38]R. M. Laszewski and P. Axel, Phys. Rev. C **19**, 342 (1979).

[39]P. P. Antropov, I. E. Mitrofanov, and V. S. Russkikh, Izv. Akad. Nauk USSR, Ser. Fiz. **34**, 116 (1969) [Bull. Acad. Sci. USSR **34**, 108 (1970)].

[40]R. R. Harvey, J. T. Caldwell, R. L. Bramblett, and S. C. Fultz, Phys. Rev. **136**, B126 (1964).

[41]L. M. Young, Ph.D. thesis, University of Illinois at Urbana-Champaign, 1972 (unpublished).

[42]R. D. Starr, P. Axel, and L. S. Cardman, Phys. Rev. C **25**, 780 (1982).

[43]J. A. Holmes, S. E. Woosley, W. A. Fowler, and B. A. Zimmerman, At. Nucl. Data Tables **18**, 305 (1976).

[44]D. S. Dale, A. M. Nathan, F. J. Federspiel, S. D. Hoblit, J. Hughes, and D. Wells, Phys. Lett. **214**, 329 (1988).

[45]R. Leicht, M. Hammen, K. P. Schelhaas, and B. Ziegler, Nucl. Phys. **A362**, 111 (1981).

[46]A. Veyssière, H. Beil, R. Bergère, P. Carlos, and A. Leprêtre, Nucl. Phys. **A159**, 561 (1970).

[47]A. Veyssière, H. Beil, R. Bergère, P. Carlos, A. Leprêtre, and K. Kernbath, Nucl. Phys. **A199**, 45 (1973).

[48]J. T. Caldwell, E. J. Dowdy, B. L. Berman, R. A. Alvarez, and P. Meyer, Phys. Rev. C **21**, 1215 (1980).

[49]G. E. Brown and M. Bolsterli, Phys. Rev. Lett. **3**, 472 (1959).

[50]U. Zurmühl, P. Rullhusen, F. Smend, M. Schumacher, H. G. Börner, and S. A. Kerr, Z. Phys. A **314**, 171 (1983).

[51]J. Speth, in *Giant Multipole Resonances*, Nuclear Science Research Conference Series, edited by F. E. Bertrand (Harwood, New York, 1979), p. 33.

[52]D. Zawischa (private communication).

[53]H. R. Kissener, I. Rotter, and N. G. Goncharova, Fortschr. Phys. **35**, 277 (1987).

[54]M. Marangoni, P. L. Ottaviani, and A. M. Saruis, Nucl. Phys. **A277**, 239 (1977). M. Marangoni and A. M. Saruis, Nucl. Phys. **A132**, 649 (1969).

[55]J. Ahrens, L. S. Ferreira, and W. Weise, in *Weak and Electromagnetic Interactions in Nuclei*, edited by H. V. Klapdor (Springer, New York, 1986), p. 167.